Journal of Molecular Liquids 439 (2025) 128862

Contents lists available at ScienceDirect

Journal of Molecular Liquids

journal homepage: www.elsevier.com/locate/molliq

Interpretation and analysis of solvent and physico-chemical parameters of choline-amino acid deep eutectic solvents and their aqueous mixtures over the kinetic response

Paola R. Campodónico *, Karla Calfuman, Cristian Suárez-Rozas, Jackson J. Alcázar, Belén Olivares

Centro de Química Médica, Instituto de Ciencias e Innovación en Medicina, Facultad de Medicina, Clínica Alemana Universidad del Desarrollo, Santiago, Chile

ARTICLE INFO

Keywords:
Green chemistry
Biocatalysis
Solvent effects
Hydrogen bonds
Amino acids
Aqueous mixtures
Enzymatic hydrolysis

ABSTRACT

This study underscores the pivotal role of choline-amino acid deep eutectic solvents, [ChCl][AA], in the hydrolysis reaction of *p*-nitrophenyl laurate (*p*-NPL), used here as a model reaction to evaluate solvent effects in various aqueous compositions. The [ChCl][AA] analyzed were choline methionine ([ChCl][Met]), and choline proline ([ChCl][Pro]). Hydrolysis reaction was performed both in the absence and presence of the enzyme *Candida Antarctica* Lipase B (CALB), allowing for detailed examination of how the reaction media influences enzymatic activity. Results indicate that varying solvent compositions significantly affect CALB's catalytic behavior. A kinetic analysis, along with physicochemical evaluations, supports these findings. Notably, in the non-enzymatic hydrolysis, [ChCl][Met] showed a rate one order of magnitude higher than [ChCl][Pro]. The concentration of the phenolate form also increased with higher molar fractions (χ) of [ChCl][AA], implying direct involvement of [ChCl][AA] in phenoxide formation. Conversely, in the enzymatic reaction, [ChCl][Pro] facilitated a rate approximately 3.5 times faster than [ChCl][Met], with rates increasing as χ increased. This effect is attributed to the rigid structure of proline, which may induce beneficial conformational changes in CALB. Lineweaver-Burk plots revealed that optimal enzymatic performance occurred in media rich in [ChCl][Met] (χ = 0.85), suggesting that such environments impose structural constraints that stabilize CALB. This stability may arise from the formation of a solvation shell near the [ChCl][AA]. Surface tension data further suggest that at specific compositions, 3D assemblies form, mimicking pure [ChCl][AA] behavior. Overall, this study emphasizes the potential of [ChCl][AA] as green solvents in biocatalysis applications.

1. Introduction

In the last time, safer solvents for chemical transformations and processes were aimed at replacing toxic volatile organic solvents (VOS), because the most of them are harmful, toxic, expensive and generate waste residues, which can cause damage to health and safety and contribute to atmospheric pollution [1,2]. The safer solvents are one of the twelve postulates designed to make chemical processes as "green" as possible by minimizing the hazards transferred to the environment through waste or other undesired products [3–5]. This new age materials generically described as *neoteric solvents [6]* include the well-known ionic liquids (IL) [7,8], and more recently the new generation of bio-based ionic liquids (BbIL) [9–15], deep eutectic solvents (DES) [16–19] and lastly the series of natural eutectic solvents (NADES) [16]. The leading property of these solvents make of them an attractive alternative in comparison to VOS is their huge combinatorial flexibility (10^{12} possible combinations), placing them as designer solvents or task-specific solvents [20] that may be used in chemical applications, biocatalysis, biological and clinical areas, catalysis and manufacturing processes [21–27].

ILs or molten salts are liquids below 100 °C, consisting mainly of organic cations with organic or inorganic anions. Due to their lower vapor pressure, they can be recyclable, but they have poor biodegradability, high toxicity and complex and expensive synthesis procedure [2,6–8]. DES have been sometimes perceived as a new class of IL analogues because they share many characteristics and properties with

* Corresponding author.
E-mail addresses: pcampodonico@udd.cl (P.R. Campodónico), cristiansuarez@udd.cl (C. Suárez-Rozas), Jackson.alcazar@udd.cl (J.J. Alcázar), molivares@udd.cl (B. Olivares).

https://doi.org/10.1016/j.molliq.2025.128862
Received 21 August 2025; Received in revised form 29 October 2025; Accepted 1 November 2025
Available online 4 November 2025

them [17]. However, it has been clarified recently that the IL and DES are two different types of solvents [18]. DES are substances formed by the combination of at least two compounds, a hydrogen acceptor (HBA) and a hydrogen-bond donor (HBD), which are typically solid at room temperature [19,27]. Finally, BbIL are a second generation of IL, containing in their chemical structure bio-compatible cations and anions from inexpensive and eco-friendly natural products such as amino acids (AA), plant-derived carboxylic acids and plant growth hormones [9–15]. These BbIL can add green features to the first generation of IL. Ohno et al. synthetized BbIL based on the 1-ethyl-3-methyl imidazolium cation and 20 AA as anions [9]. These were clear liquids that were thermally stable, cheaper, biodegradable, and more biocompatible than previous ILs [9,10], but obviously, the cation was not biobased. DES based on choline-amino acids defined as [ChCl][AA] were introduced by Liu in 2012 [28,29]. The [ChCl][AA] are biodegradable and show less toxicity [30]. Moreover, [ChCl][AA] can be prepared from natural and renewable feedstocks, improving its green features compared to ILs [2].

IL and DES and their aqueous mixtures are been investigated as promising reaction media in different fields [19,23]. To date, [ChCl][AA] and its aqueous media have been less explored as a reaction media, opening a significant debate about the amount of water tolerated and the effect of water molecules over the [ChCl][AA] and/or the water molecules over the moieties of [ChCl][AA] [2,31]. Then, the water effects over the [ChCl][AA] must be analyzed, considering the correlation between its physicochemical properties and solvent effects to analyze each reaction media's supramolecular structure and properties.

This study considers three (3) [ChCl][AA] based on choline chloride (ChCl) and methionine (Met), alanine (Ala), and proline (Pro), respectively. (See Scheme 1 below). Note that the acronyms used in this study include [ChCl][Met] (choline chloride-methionine), [ChCl][Ala] (choline chloride-alanine) and [ChCl][Pro] (choline chloride-proline), respectively.

This work evaluated the performance of these [ChCl][AA] and their aqueous mixtures at different molar fractions (χ). The role of water must be analyzed considering its effect on the physicochemical properties and its effect on the [ChCl][AA] components due to the water could strongly interact with the [ChCl][AA] network because it is possible that water molecules change the network. In order to resolve this controversy, this study considers the mentioned [ChCl][AA] and their aqueous mixtures, which were analyzed across physicochemical parameters, including conductivity, density, surface tension and solvatochromic solvent parameters. These parameters will be evaluated over the kinetic response in each reaction media to identify the main specific microscopic interactions responsible for the observed kinetic response. Therefore, the benchmark system used to evaluate the solvent effects will be a nucleophilic reaction, which is involved in a catalytic process (See Scheme S1 in Supporting Information (SM)) because these reaction media will play a key role in biocatalysis processes. This reaction corresponds to the hydrolysis of the substrate *p*-nitrophenyl laureate (*p*-NPL) mediated by *Candida Antarctica* Lipase B (CALB). CALB is a suitable enzyme model for studying solvent effects because it is a very stable enzyme compared to other lipases [23,32–34]. The kinetic analysis will highlight the pivotal role of the environment's polarity over the solvent's first shell [35] because the enzyme hydration and the solvation of the enzyme and the substrate must be considered. This study is centered on the analysis of each reaction media over the rate coefficient values, which is a mainly unstudied open area to be explored. This study suggests a promising approach for potential applications and further perspectives on green industrial solvents.

2. Materials and methods

2.1. Materials

Choline chloride (purity ≥99 % (thin layer chromatography, TLC) and water content ≤5 %), L-methionine ((2*S*)-2-amino-4-(methylsulfonyl) butanoic acid, purity ≥99 %), L-alanine (2-aminopropionic acid, purity >98.5 %), L-proline ((2*S*)-pyrrolidine-2-carboxilic acid, purity ≥99 %), potassium hydroxide (purity ≥100 %), ethanol (EtOH, purity ≥100 %), methanol (MeOH, purity ≥100 %), acetonitrile (MeCN, purity ≥100 %), *p*-NPL (purity ≥98 % (gas chromatography, GC)), *para*-nitrophenol (*p*-NP, purity ≥99 % (GC)), N,N-diethyl-4-nitroaniline (purity ≥99 % (GC)), *para*-nitroaniline (purity ≥99 % (GC)), Reichardt's dye content 90 %, Nile red, were purchased from Sigma. The salts, KH_2PO_4 and K_2HPO_4, were acquired from Merck (purities (alkalimetric assay) > 99.5 %). All reagents were used as soon as delivered. For the preparation of the aqueous solutions used, ultrapure water was used (Merck-Millipore Simplicity™ ultraviolet, UV water purification system). CALB was purchased from Sigma Aldrich as lipase from *Candida Antarctica* (lyophilized powder). Water standard 1 %, certified reference material for Karl Fisher titration, titrant 5 for volumetric Karl Fisher titration with two component reagents (contains methanol, iodine) and solvent for volumetric Karl Fisher titration with two component reagents (contains methanol, imidazole).

2.2. Preparation of choline-amino acid deep eutectic solvents

The preparation of [ChCl][Met], [ChCl][Ala], and [ChCl][Pro]) was achieved through a neutralization reaction, based on the procedure described by Gaikwad and co-workers with slight modifications (see Scheme S2 in the SM) [13,14]. Briefly, in a dry 250 mL single-neck round-bottom flask, KOH (1.00 equiv.) was added. The flask was purged with N_2, EtOH (1.00 equiv.) was added using a syringe, and the mixture was stirred at room temperature for 3 h. After this time, the resulting solution was added to a mixture of the HBA (choline chloride; 1.00 equiv.) and the HBD (amino acids: L-methionine, L-alanine, or L-proline; 1.00 equiv.). The flask was purged again with N_2, and the mixture was stirred at room temperature for 48 h. Then, the resulting mixture was filtered, the precipitate was washed with cold EtOH, and the obtained solution was concentrated under reduced pressure at 55 °C for at least 1 h to eliminate solvent traces. Finally, a gentle N_2 stream was applied, and the resulting [ChCl][AA] were stored at 4 °C. It is worth noting that each synthesized [ChCl][AA] was monitored for at least one week, and only those showing no apparent changes in physical characteristics (e.g., opacity, precipitation) were used in further studies.

2.3. Spectroscopic characterization (^{1}H NMR) of synthesized choline-amino acid deep eutectic solvents

The identity and purity of the synthesized [ChCl][AA] ([ChCl][Met], [ChCl][Ala], and [ChCl][Pro]) were confirmed by proton nuclear magnetic resonance, ^{1}H NMR spectroscopy. NMR spectra were recorded on a

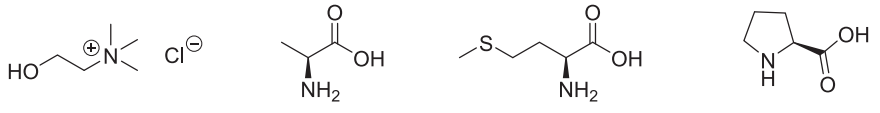

Choline Chloride (ChCl) **L-alanine (Ala)** **L-methionine (Met)** **L-proline (Pro)**

Scheme 1. Structures of [ChCl][AA] used in this study.

Bruker Avance 400 MHz spectrometer. All chemical shifts in NMR experiments are reported in ppm downfield from tetramethylsilane, TMS. The following calibration was used: D_2O $\delta = 4.79$ ppm for ^1H NMR. Coupling constants (J) are given in Hertz (Hz), and the following abbreviations are used to describe the signal multiplicity: s (singlet), bs (broad singlet), d (doublet), dd (doublet of doublets), t (triplet), td (triplet of doublets), q (quartet), quint (quintet), and m (multiplet). All NMR spectra were processed and analyzed using MestRe Nova 14.1.2. The observed signals for each compound are consistent with those previously reported in different literature sources, confirming the successful formation of the corresponding [ChCl][AA] (full spectra are available in Figs. S1–S3 in the SM).

[ChCl] [Met]: ^1H NMR (400 MHz, D_2O) δ 4.12–4.03 (m, 2H), 3.57–3.50 (m, 2H), 3.34 (t, $J = 6.3$ Hz, 1H), 3.22 (s, 9H), 2.58 (t, $J = 7.8$ Hz, 2H), 2.14 (s, 3H), 2.02–1.76 (m, 2H). The spectral data matched that previously published [14,36].

[ChCl] [Ala]: ^1H NMR (400 MHz, D_2O) δ 4.12–4.03 (m, 2H), 3.56–3.50 (m, 2H), 3.42–3.29 (m, 1H), 3.22 (s, 9H), 1.24 (d, $J = 6.9$ Hz, 3H). The spectral data matched that previously published [14,36].

[ChCl] [Pro]: ^1H NMR (400 MHz, D_2O) δ 4.11–4.01 (m, 2H), 3.55–3.46 (m, 3H), 3.20 (s, 9H), 3.05 (dq, $J = 12.6$, 6.6, 6.0 Hz, 1H), 2.78 (dt, $J = 11.3$, 6.3 Hz, 1H), 2.20–2.03 (m, 1H), 1.74 (dq, $J = 11.1$, 6.5, 5.6 Hz, 3H). The spectral data matched that previously published [14,36].

2.4. Aqueous mixtures of choline-amino acid deep eutectic solvents

This study used pure water and [ChCl][AA] mixtures in a wide-range of χ concerning [ChCl][Met] and [ChCl][Pro], respectively. Each mixture was prepared by weighting the amount of [ChCl][AA] and water into a screw-capped vial in an analytical balance (RADWAG AS 220.R2). To favor mixing, each mixture was shaken for 1 min, then left to equilibrate overnight before use in order to equilibrate the mixture. All of the studied mixtures appeared homogeneous after this treatment, except [ChCl][Ala]/water mixtures which showed a precipitate of white color. (See Fig. S4 in SM for more details). The rheological properties of the [ChCl][AA] were modified by changing the quantity of water, resulting in solvents with varying viscosities ranging from clear fluid liquids to a clear viscous phase. Note that, all these mixtures were used on the kinetic study and the solvent effects analysis. Then, these mixtures were used only in some analysis based on their rheological features [19,23].

Hydrolysis Reaction of *p*-nitrophenyl laureate in Choline-Amino Acid Deep Eutectic Solvents.

The investigated reaction corresponds to hydrolysis of the substrate *p*-NPL in each reaction medium. (See Scheme S1 in SM without CALB). The analyzed aqueous mixtures are from [ChCl][Met] and [ChCl][Pro], respectively. The kinetic of the reaction was performed spectrophotometrically at $\lambda = 400$ and 260 nm using a diode array spectrometer UV–Vis Agilent 8453 connected to a recirculatory water bath at 25 °C. All the reactions were studied under excess nucleophile (water) over the substrate (at least 10 times greater than the substrate concentration) in order to stablish the pseudo-first-order kinetics. The kinetic study started by injecting the substrate stock solution in acetonitrile (10 μL, [53.89] mM) into the 940 μL of each reaction media (1 mL in the spectrophotometric cell). The formation of the colored kinetic product (*p*-NP) was monitored by UV–vis spectrophotometry at $\lambda = 410$ nm. On the other hand, the decay of *p*-NPL was monitored by UV–vis spectrophotometry at $\lambda = 260$ nm. In all the runs, the pseudo-first-order rate coefficients (k_{obs}) were found for all the reactions. The k_{obs} values were determined by means of the spectrophotometric kinetic software for the first-order reactions at the wavelength corresponding to the kinetic product. Then, the relationships between k_{obs} vs. χ (wide-range with respect to BbIL) should be straight lines or straight lines with smooth deviations, which will discard a catalysis process by the media. The k_N value is obtained from a plot in accordance with Eq. 1:

$$k_{obs} = k_0 + k_N[Nu] \quad (1)$$

where k_0 is the rate coefficient for the solvolysis, [Nu] is the concentration of nucleophile and k_N is the rate coefficient of the nucleophilic attack of the substrate. The kinetic methodology was taken from previous kinetic studies cited in literature and previous works performed by our group. [37] Note that, k_0 is discarded and $k_N$is the rate coefficient for the hydrolysis (nucleophilic attack) and the concentration of nucleophile is expressed by χ [38]. See Tables S1 to S4 and Figs. S5 and S6 in SM for more details.

2.5. Lipase activity assays in choline-amino acid deep eutectic solvents

This study used [ChCl][Met] and [ChCl][Pro] and their water mixtures in a wide-range of χ. The substrate solution (*p*-NPL) was prepared in MeCN at 58 mM. The enzymatic solution was prepared by adding 10 mg by 1 mL of potassium phosphate buffer solution. Lipase activities were carried out by UV–vis spectrophotometry using an Agilent 8453 UV–Vis spectrometer connected to a recirculatory water bath at 25 °C. Aliquots from a stock solution (10 μL) of *p*-NPL were added to 1 mL each reaction media containing the enzyme (aliquots from a stock solution (20 μL) of lipase). Release of *p*-NP was recorded by following the increase in absorbance at 410 nm. Initial reaction rates were calculated during the first 150 s of the initial segment of the reaction profiles according to eq. 2 [26,34,38]:

$$v = \frac{k_{cat}[E_0][S]}{K_M + [S]} \quad (2)$$

where v corresponds to the rates of CALB catalyzed hydrolysis of *p*-NPL. $[E_0]$ is the enzyme concentration used in the hydrolysis experiments, [S] corresponds to the substrate concentration at which the associated reaction rate was determined, k_{cat} corresponds to the rate coefficient defined as k_2 (ES → P, see more details in Scheme S3 in SM, where ES and P correspond to enzyme-substrate complex and the product) and K_M is the Michaelis constant from the Michalis-Menten equation [19,23]. See Tables S5 to S8 and Figs. S7 to S8 in SM for more details and section 3.3.3 Lineweaver-Burk Relationships in the text.

2.6. Product analysis

Product authentication was performed following the increase of the absorption band centered in 400 nm attributable to the corresponding reaction product of the hydrolysis reaction (*p*-NP, see Scheme S1 in SM) [19,23,32,37]. On the other hand, the kinetic decay follows the decomposition of *p*-NPL through its absorption band centered at 260 nm. More details in SM, Fig. S9.

2.7. Electric conductivity measurements in choline-amino acid deep eutectic solvents

The conductivity of the samples was measured at room temperature using an AD3000 EC/TDS Temperature Meter provided with a 4-pole conductivity probe, expressed in ($\frac{mS}{cm^{-1}}$) within an uncertainty of ± 0.01 ($\frac{mS}{cm^{-1}}$). All measurements were.

performed in duplicate, see SM for more details [17,23,32,39]. See Tables S9 and S10 in SM for more details.

2.8. Viscosity measurements in choline-amino acid deep eutectic solvents

Viscosity parameter (δ) expressed in (mPa • s) was used to characterize the reaction media and to evaluate their effects on the enzymatic reactions. The dynamic viscosities were measured at 25 °C using a rotational viscometer (Fungilab Viscolead series) connected to a recirculatory water bath. Each measurement was performed in duplicate for

each studied reaction media, see SM for more details [39,40]. See Tables S11 and S12 in SM for more details.

2.9. Density measurements in choline-amino acid deep eutectic solvents

The density parameter (ρ) of each studied reaction media expressed in (g/mL) were determined by using an Anton Paar Density Meter Instrument DMA 35 at room temperature. Each measurement was performed in duplicate for each studied reaction media, see SM for more details [19]. See Tables S13 and S14 in SM for more details.

2.10. Solvatochromic solvent parameters in choline-amino acid deep eutectic solvents

The Kamlet Taft correlation quantifies solute-solvent interactions defined as specific (HB or donor-acceptor interactions) and non-specific (polarity/polarizability) effects. This scale considers 4 chromophores to evaluate the solvent properties; Reichardt dye (RD), N,N-diethyl-4-nitroaniline (B), *p*-nitroaniline (C), and Nile red (NR). [19] (See Scheme S4 in SM). These solvatochromic probes undergo spectral shifts making it possible to determine the nature of the solvent in the solvation shell using eqs. 3 to 7 below. These parameters were measured by injecting the reaction media (950 μL) into a quartz cuvette with an optical path of 1 cm with the probes, previously prepared in methanol. Note that, 50 μL of the stock solution of each probe was evaporated to dryness for 30 min in a rotary evaporator Buchi R-300. The concentration of stock solution of each probe was 1.85×10^{-3} M. Each reaction media was thermostated at 25 °C and measured using a UV–vis spectrophotometry Agilent 8453 UV–Vis spectrometer [6,19,23,41]. Each measurement was performed in duplicate for each studied reaction media. See Tables S15 to S25 in SM for more details.

$$ET_{30} = \frac{28591}{\lambda_{max}\,(RD)} \tag{3}$$

$$\pi^{*} = 0.314\,(27.52 - \nu_B); \tag{4}$$

$$\alpha = 0.0649\,ET_{30} - 2.03 - 0.72\pi^{*} \tag{5}$$

$$\beta = \frac{(1.035\,\nu_B + 2.64 - \nu_C)}{2.80} \tag{6}$$

$$E_{NR} = \frac{1.196 \text{ x } 10^5}{\lambda_{max}(NR)} \tag{7}$$

2.11. Karl fischer method

The measurements were performed in a Hanna HI 933–02 Karl Fischer Volumetric Titration apparatus. This titration was used to obtain reference water concentration. Karl Fisher titrations were carried out filling the beaker titration up with solvent (50 mL). The syringe is filled and needled with the sample. Then, it is weighted and added the sample to the beaker titration. The syringe is weighted again in order to determine the added sample mass (by difference of the two measurements). The exact weight is entered in order to start the analysis. Then, for this study, the water concentration determinates for [ChCl][Met]was of 10.90 %w/w in water (10.6 and 11.2 %w/w in water) [19]. Note that, the studied reaction medias will contain a certain amount of water which can be considered as an impurity specially in hydrophilic systems even if they are dried [19]. On the other hand, the water concentration determinates for [ChCl][Pro]was of 10.6 %w/w in water (10.01 and 11.1 %w/w in water). Finally, the water concentration determinates for [ChCl][Ala]was of 6,48 %w/w in water (6.91 and 6.05 %w/w in water).

2.12. Surface tension measurements in choline-amino acid deep eutectic solvents

Surface tension (SFT) measurements were conducted using a Dataphysics DCAT 9 T tensiometer equipped with a Du Noüy ring RG 11, fabricated from platinum–iridium in accordance with DIN 53914 standards. The sample vessel was filled with the test solution and placed into the DCAT apparatus. Subsequently, the ring was mounted onto the probe holder to record the SFT values. The SFT were measured at 21°C using the tensiometer connected to a recirculatory water bath. All measurements were performed in duplicate for each reaction medium under investigation (refer to Table S26 in SM for further details). The aqueous mixtures analyzed consisted of [ChCl][Met] and [ChCl][Pro], at mole fractions (χ) of 0.25, 0.50, 0.75, and 1.0, respectively. Note that, the SFT for pure water was 69.16 mN/m (69.45 ± 0.43 mN/m and 68.86 ± 0.41 nM/m).

3. Results and discussion

3.1. Solvent effects parameters

In order to examine the solvent effects each [ChCl][AA] were analyzed in great detail to consider the physicochemical and solvent effects parameters. This study used [ChCl][Met] and [ChCl][Pro] and their water mixtures in a wide-range of χ. Note that, [ChCl][Ala] was synthetized. However, it is a solid at room temperature and its aqueous mixtures are not stables, showing a white precipitate (see Fig. S4 in SM). For this reason, [ChCl][Ala] and its aqueous mixtures were not considered in this analysis. Fig. S2 (in the SM) indicates the formation of [ChCl][Ala], and Fig. S4 (in the SM) displays its aqueous solution at χ = 0.1, which corresponds to a high-water content relative to [ChCl][Ala]. This observation reflects the low solubility of [ChCl][Ala] in water. The limited solubility may be ascribed to the relatively polar character of the DES compared to water. Scheme 1 presents the general structures of the constituent molecules of [ChCl][AA]. The L-alanine moiety includes a methyl substituent (an electron-donating group) adjacent to the amino group (–NH_2), which may interfere with the HB network by perturbing the electron distribution around nearby atoms and thus altering the proton affinities of functional groups participating in HB. Such perturbation can lead to a weaker, less stable, or otherwise modified network relative to an analogous system lacking the methyl substituent, thereby influencing the overall structure and stability of biomolecules such as peptides and proteins when it acts as reaction media [42]. Then, to investigate solvent effects and to get physico-chemical parameters, it is essential that the reaction medium remains homogeneous. Then, a complete study of basicity based on Kamlet-Taft (KT) model was performed for [ChCl][Met] and [ChCl][Pro] and their water mixtures in a wide-range of χ with respect to [ChCl][Met] and [ChCl][Pro], respectively. Details are available in SM, in Tables S15 to S25).

Fig. 1 shows the relationships between β parameter of KT model vs. χ of [ChCl][Met]/water mixtures (full squares) and [ChCl][Pro]/water mixtures (empty squares). The β parameter, is related to the ability of the solvent to accept hydrogen bond (HB) [43,44]. See Eq. 6 in section 2.11 in the text. Note in the first part of Fig. 1 for [ChCl][Met] and its water mixtures, the β values increase upward with rising molar fraction of [ChCl][Met]. This fact suggests that previous χ = 0.40 there is a competition between the water molecules and the [ChCl][Met] moieties to stablish HB. Therefore, the first part of this Figure could be defined as a basic range or HBA. However, if the amount of [ChCl][Met] increases in the mixture (χ > 0.40), the effect increases which is associated to a lower degree of freedom of the water molecules (low quantity) and the saturation of sites to bond by the [ChCl][Met] moieties. This plot suggests the transition states from the solvated [ChCl][Met] moieties to the [ChCl][Met] network formation excluding the water molecules acting as solvation of the stablished network. On the other hand, [ChCl][Pro] and

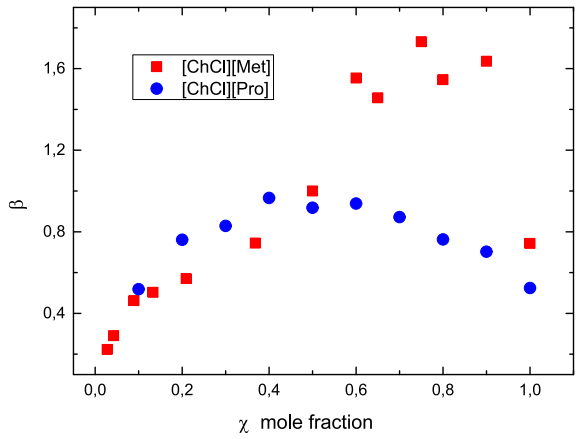

Fig. 1. Relationship between β vs. χ of [ChCl][Met]/water mixtures (full squares) and [ChCl][Pro]/water mixtures (empty squares), respectively.

its water mixtures (Fig. 1, empty squares) shows a smooth increase and decrease in comparison to [ChCl][Met] plot. Then, mixtures [ChCl][Met] shows a bigger trend to accept HB (after $\chi > 0.5$) in comparison to [ChCl][Pro]. This fact could be related to the chemical structure of L-methionine and L-proline and their groups to stablish HB with water molecules. (See Scheme 1 above).

Fig. 2 shows the relationship between α parameter of KT model vs. χ for [ChCl][Met]/water mixtures (full squares) and [ChCl][Pro]/water mixtures (empty squares). The α parameter is related to the ability of the solvent to donate HB [43,44]. See Eq. 5 in section 2.11 in the text. This Figure shows 3 defined zones for [ChCl][Met]. First, χ between 0.0 and 0.4 shows a lower ability of the reaction media to donate a HB to the probe. This range rich in water molecules are suggesting the solvation of the [ChCl][Met] moieties. However, this parameter increases drastically between χ of 0.4 to 0.6, suggesting that the region associated with a minor quantities of water molecules are establishing a strong network by HB interactions between the reacting pairs and [ChCl][Met], increasing the possibility of donating HB in order to stablish a network of [ChCl][Met]. Then, the last part of this Figure suggests a χ range able to stablish HBD between the [ChCl][Met] denoting a constant value, proposing a [ChCl][Met] network stablished since $\chi > 0.65$. Note that, [ChCl][Pro] and its water mixtures (Fig. 2, empty squares) shows a low constant value in all the studied mixtures, denoting a low ability of the solvent to donate HB.

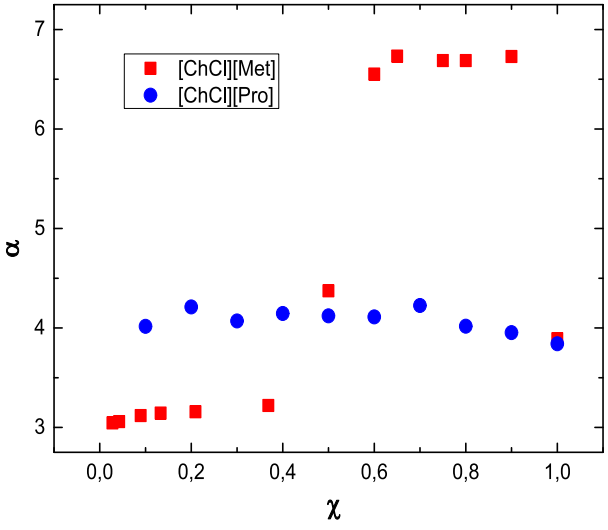

Fig. 2. Relationship between α vs. χ of [ChCl][Met]/water mixtures (full squares) and [ChCl][Pro]/water mixtures (empty squares), respectively.

Fig. S10 in SM shows the relationships between NR parameter of KT model vs. χ of [ChCl][Met]/water mixtures (full squares) and [ChCl][Pro]/water mixtures (empty squares). NR is a neutral solvatochromic dye that exhibits a large positive solvatochromism, going from non-polar to polar reaction media [43–45]. See Eq. 7 in section 2.11 in the text. Then, NR displays increasing red shifts in both absorption and emission wavelength as the solvent polarity is increased. Fig. S10 for both studied mixtures indicate different environments, where the polarity increases until $\chi = 0.5$, attributable to a range rich in HB interactions. Then, it diminishes its polarity until to reach a constant value close the [ChCl][AA] pure. On the other hand, Fig. S11 in SM shows the relationships between ET30 parameter of KT model vs. χ of [ChCl][Met]/water mixtures (full squares) and [ChCl][Pro]/water mixtures (empty squares). See Eq. 3 in section 2.11 in the text. Note that, the polarity of [ChCl][Met] and its mixtures is constant between 0.1 and 0.4 of molar fraction, showing a low value. In this range of composition, the protonated dye lost its capacity as polarity dye. Then, it increases until to reach a plateau close to [ChCl][Met] pure. On the other hand, [ChCl][Pro] and its water mixtures (Fig. S11, empty squares) shows a high value constant in all the studied mixtures. In acid media, NR does not lose its solvatochromic behavior, in contrast with the ET30 dye [27]. In these instances, NR is completely complementary to ET30. Then, the relationship between ET30 vs. NR is showed in Fig. 3 for [ChCl][Met] and its water mixtures. In it is observed 2 strong ranges of compositions with different polarities (χ between 0.1 and 0.5 and χ between 0.5 and 0.9, respectively).

Fig. 4 shows the relationships between π^* (dipolarity-polarizability) parameter of KT model vs. χ of [ChCl][Met]/water mixtures (full squares) and [ChCl][Pro]/water mixtures (empty squares). See Eq. 4 in section 2.11 in the text. For [ChCl][Met], in the first part, mixtures rich in water molecules show a high parameter until $\chi = 0.4$. Then, it decreases to $\chi = 0.4$ with the addition of [ChCl][Met] and then it is maintained constant close to [ChCl][Met] pure. Note that, π^* also increases with increasing β in the range between 0 and 0.4 of molar fractions, which indicates that the distance of the [ChCl][Met] moieties is increased by maintenance of the charges of the components of the [ChCl][AA]. This result is interpreted in such a way, that a clear effect of dipolarity occurs rather than of polarisability. While, [ChCl][Pro] shows a constant and high value of π^* parameter in all the studied range.

All these parameters are suggesting that at the first region, rich in water molecules, the reactants that form the [ChCl][AA] are completely solvated with high formation of HB between them with the water molecules. As the [ChCl][AA] increases in composition of AA, is observed a change that ends with a range close to [ChCl][AA] pure. This fact suggests that the water molecules are occluded in the [ChCl][AA] network, or these molecules are externally solvating the [ChCl][AA]. Note that, at

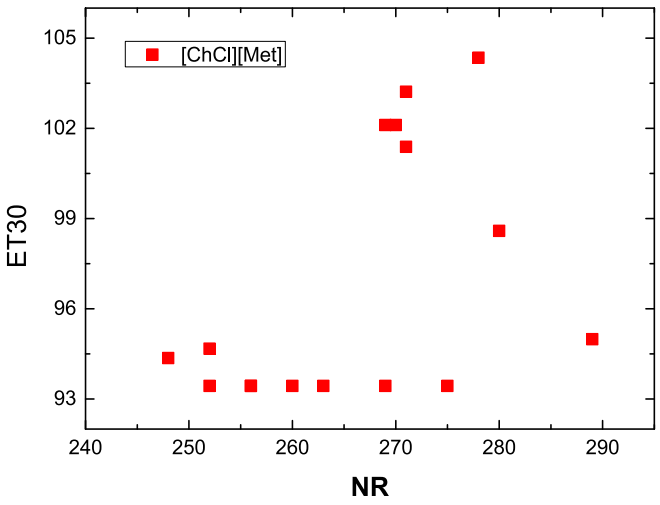

Fig. 3. Relationships between ET30 vs. NR of [ChCl][Met]/water mixtures.

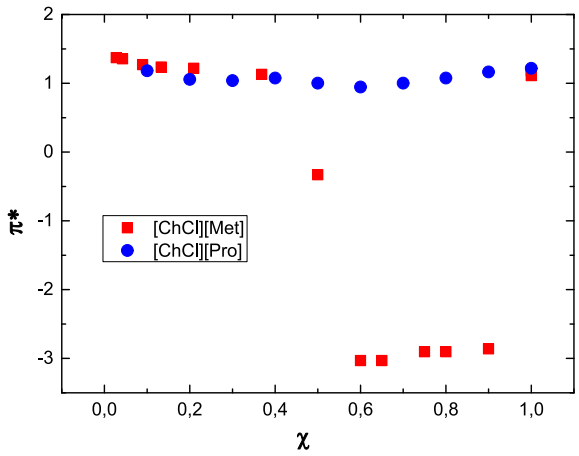

Fig. 4. Relationships between π^* vs. χ of [ChCl][Met]/water mixtures (full squares) and [ChCl][Pro]/water mixtures (empty squares), respectively.

$\chi > 0.4$ the behavior for [ChCl][Met] is similar to the [ChCl][AA] pure. It is noteworthy that both [ChCl][AA] exhibit distinct solvatochromic behaviours, indicating the presence of two unique solvation environments influenced by their respective compositions and intermolecular interaction forces.

3.2. Physico-chemical parameters

Fig. S12 shows the relationships between density vs. χ of solvent mixture. Full squares are associated to [ChCl][Met] and its water mixtures and empty squares to [ChCl][Pro] and its water mixtures, respectively. The trend associated to [ChCl][Met] shows two zones strongly demarcated. The first one is a zone rich in water at the range of compositions between 0.0 and 0.4 of molar fraction, characterized by strong variations in this narrow range of compositions. The second zone associated to this Figure corresponds to a plateau, suggesting that the density values would be independent of the composition of the solvent mixture. Note that, for each mixture where the density parameter is increasing (first zone), suggests greater movements and the development of charges and higher abilities to establish HB. Then, at those compositions, the interactions between HBA and HBD should be broken, suggesting aqueous solutions of the single [ChCl][AA] components. This fact suggests a competition between the water molecules and the [ChCl][AA] moieties to stablish an HB. On the other hand, if the amount of [ChCl][Met] increases in the mixture ($\chi > 0.4$), the effect is constant due to a lower degree of freedom of the water molecules to bond the [ChCl][Met] moieties and a region with a three-dimensional (3D) network stablished for the [ChCl][AA]. Note the relationship with β parameter (see Fig. 1 above). The density parameter varies softly with the compositions. On the other hand, empty squares are associated to [ChCl][Pro] and its water mixtures. This trend shows a zone rich in water molecules where it decreases at the range of compositions between 0.1 and 0.3 of molar fraction suggesting a high separation between [ChCl][Pro] moieties with a great number of interstices or spaces in the 3D network. Then, this trend increases slightly until reaching a plateau, suggesting that the water molecules will be stablishing a solvation box close to the [ChCl][AA] formed. (See Scheme 5 in SM for more details). Scheme S5 shows a general picture for [ChCl][Met] and some interactions and solvation patterns. On the other hand, Fig. S13 shows the relationship between conductivity and different molar fractions for both studied [ChCl][AA]. (Full squares for [ChCl][Met] and empty squares for [ChCl][Pro] and their aqueous mixtures, respectively). Note that, both show the same trend. The conductivity parameter is low and constant in zone rich in water molecules. Then, it suffers an abrupt increasement at the range of compositions between 0.45 and 0.65. Finally, this parameter decreases as the composition of [ChCl][AA] is major. Note that, these high values are associated with the previous range of composition to reach the plateau in the density parameter. Note in Fig. S13 that, both trends exhibit changes in their slopes, indicating alterations in the nature of the mixtures. These changes suggest the formation of [ChCl][AA] networks and modifications in solvation patterns; at low χ values, the constituent moieties of [ChCl][AA] are likely extensively solvated by the large excess of water, implying a high degree of freedom for each component of [ChCl][AA]. In regimes characterized by low water content, interactions between [ChCl][AA] species predominate, with water molecules merely surrounding the [ChCl][AA] network. At intermediate water concentrations, pronounced structural transitions occur water molecules begin to penetrate the network, establishing bridges of [ChCl][AA]–water–[ChCl][AA] interactions [19].

Fig. S14 in SM shows the relationship between viscosity and its different molar fractions for both studied [ChCl][AA]. Full squares for [ChCl][Met] and empty squares for [ChCl][Pro], respectively. Note that, both show a similar trend. These trends increase directly with the water content in the compositions toward pure [ChCl][AA].

Fig. 5 illustrates the relationship between surface tension (SFT) and its different molar fractions for both studied [ChCl][AA]. Full squares represent [ChCl][Met] and empty squares correspond to [ChCl][Pro], respectively. Notably, both [ChCl][AA] exhibit similar trends, however, [ChCl][Pro] displays slightly lower values compaed to [ChCl][Met]. These trends exhibit a decreasing pattern and converge as the composition approaches that of the pure [ChCl][AA].

SFT denoted by (γ) is defined as the tendency of the fluid to minimize its surface area to the greatest extent possible [46,47]. According to our findings, the main factor influencing the SFT of the aqueous mixtures of [ChCl][Met] and [ChCl][Pro] are the composition of the mixtures and the intermolecular interactions stablished among the HBD, HBA and/with the water molecules. As shown in Fig. 5, SFT values of pure [ChCl][AA] are significantly lower than that observed in their aqueous mixtures with elevated water content (see Fig. 5). It is noteworthy that the relationships between SFT and ln (χ) were employed to determine the critical concentration of each [ChCl][AA] studied (see Figs. S15 A and B in SM, for more details). The resulting values for [ChCl][Pro] and [ChCl][Met] were approximately $\chi = 0.606$ and $\chi = 0.427$, respectively. These findings suggest that, at the examined molar fractions, the [ChCl][AA] are primarily stabilized by hydrogen bonding interactions with water molecules surrounding the [ChCl][AA] assemblies as they begin to form 3D network structures. The area under the curve for the first linear segment (mole fraction range 0.1 to 0.5 in Fig. S15) exhibits a

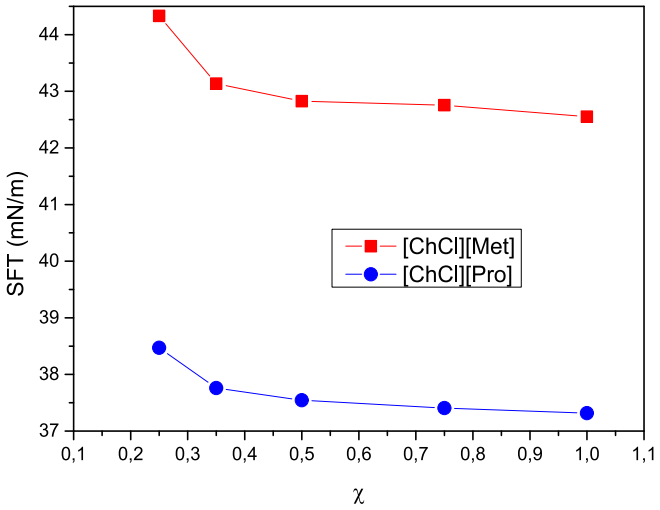

Fig. 5. Relationships between surface tension vs. χ of solvent mixture of [ChCl][Met]/water mixtures (full squares) and [ChCl][Pro]/water mixtures (empty squares), respectively.

pronounced slope compared to that of the second line, reflecting how surface tension decreases as the mole fraction of [ChCl][AA] increases. Accordingly, the addition of [ChCl][AA] behaves more like a surfactant than water: as its concentration increases, surface tension declines, which implies that [ChCl][AA] molecules accumulate and adsorb at the liquid–air interface, thereby weakening the cohesive forces among water molecules. This study consolidates physicochemical parameters and kinetic analyses. Surface tension measurements have been evaluated alongside other obtained parameters. However, an investigation into the surface tension of binary or ternary mixtures should be complemented with a comparative approach to validate the accuracy of surface tension data using the Gibbs adsorption isotherm and the linear form of the Langmuir adsorption isotherm [48].

Note that, at these molar fractions, each [ChCl][AA] exhibits an increase in conductivity, reaching a plateau (see Fig. S12 in SM), while the conductance also increases (see Fig. S13 in SM). Furthermore, Fig. 1 shows that the β parameter of the KT model reaches its maximum values, suggesting that the functional groups of methionine and proline are involved in HB interactions. This fact could be explained because DESs have been employed in aqueous two-phase systems (ATPS). However, ATPS display non-stoichiometric partitioning between the two aqueous phases for the hydrogen bond acceptor (HBA) and the hydrogen bond donor (HBD) constituting the DES [49]. Studies based on pH variation suggest that the partitioning mechanism is strongly influenced by changes in the DES moieties and is largely governed by differences in hydrophobicity between the phases [50]. Choline chloride (ChCl), a quaternary ammonium salt comprising a choline cation and a chloride anion, is commonly used as the HBA in DES formulations. Although ChCl cannot undergo proton transfer due to its quaternary ammonium structure, proton redistribution within the HB network - especially in the presence of water - contributes to the dynamic equilibrium characteristic of DES systems. Consequently, the partitioning into aqueous phases may primarily reflect the dominance of solvation effects [51].

The measured pH [52] values of **[ChCl] [Met]** and **[ChCl] [Pro]** and their aqueous mixtures are presented in Table S27 of the Supplementary Material and indicate a basic environment. Notably, the basic pH increases proportionally with the molar fraction of **[ChCl] [AA]**, plateauing at approximately $\chi = 0.5$. Under basic conditions, deprotonation of the amino acid (AA) to its anionic form ($-CO_2^-$ and $-NH_2$) is favored. In this context, water molecules may solvate these anions via hydrogen bonding: one plausible interaction is an HBD between the oxygen atom of water and the amino hydrogen of the AA, and another is an HBA between the hydrogen of water and the oxygen atom of the AA. This interpretation aligns with Figs. 1 and 2, which illustrate the solvent's capacity to donate and accept hydrogen bonds. It is worth noting that **[ChCl] [Met]** demonstrates a higher hydrogen-bonding capability relative to **[ChCl] [Pro]**, likely attributable to its more open molecular structure and functional groups (see Scheme 1). Moreover, these solvent parameters show a correlation with observed rate constants (See Tables S1, S2, S5, S6 and S27 in the next section).

In summary, the physicochemical parameters revealed distinct differences between [ChCl][Met] and [ChCl][Pro]. At low concentrations of [ChCl][AA], enhanced molecular mobility and charge development were observed, along with an increased capacity for hydrogen bond (HB) formation. As the [AA] content in the mixture increases, a region characterized by the establishment of a three-dimensional (3D) network structure of [ChCl][AA] emerges. This structural transition is corroborated by changes in conductivity and surface tension measurements, as indicated by variations in their slopes, reflecting modifications in the nature of the mixtures.

3.3. Kinetics

3.3.1. Hydrolysis reaction in choline-amino acid deep eutectic solvents

The kinetic analysis of the hydrolysis reaction of *p*-NPL in [ChCl][Met] (full squares) and [ChCl][Pro] (empty squares) and their water mixtures in a broad range of χ without CALB at 25 °C is shown in Fig. 6. This Figure shows the relationships between k_{obs} vs. χ at 400 nm. The kinetic product corresponds to the formation of phenoxide mediated by the water molecules from *p*-NPL (see Scheme S1 in SM), where the k_N value is 0.082 ± 0.004 with $R^2 = 0.973$ in the range of studied χ for [ChCl][Met] and its water mixtures. Note that, $\chi = 1.0$ was discarded attributable to a reaction media highly viscous. On the other hand, the kinetic product for [ChCl][Pro] and its water mixtures in a broad range of χ without CALB at 25 °C showed a k_N value of 0.0669 ± 0.004 with $R^2 = 0.967$ in the range of studied χ. Note that, both trends show the same behavior being the hydrolysis reaction of *p*-NPL in [ChCl][Met] one order of magnitude higher in comparison to [ChCl][Pro], and the [phenolate form] increases with χ in agreement to the increase of [ChCl][Met] in the mixture (see Fig. S5 in SM). This fact suggests that [ChCl][Met] will participate in the reaction of phenoxide formation. L-methionine shows relevant HBD and HBA sites in its chemical structure such as: -amino, carboxylic and sulfhydryl groups (see Scheme 1 above) able to interact with water molecules to promote the *p*-NP formation.

Fig. S6 (A and B) show the relationships between $\boldsymbol{k_{obs}}$ vs. χ at 260 nm for the range of χ described above at 25 °C. Figs. S6 show the decay of *p*-NPL in both reaction media and their aqueous mixtures for [ChCl][Met] (Fig. S6 A) and [ChCl][Pro] (Fig. S6 B), respectively. For values of χ between 0.1 and 0.5 the decay of *p*-NPL will be associated to the presence of high quantities of water molecules in the reaction media. Then, the χ range between 0.5 and 1.0 suggests that the decay of *p*-NPL is negligible. However, the hydrolysis reaction is high (see Fig. 6 above), suggesting that the [ChCl][AA] will be participating in this reaction.

3.3.2. Enzymatic reaction in choline-amino acid deep eutectic solvents

The study considered the kinetic analysis of the hydrolysis of *p*-NPL in presence of CALB in both studied [ChCl][AA] and their water mixtures in a broad range of χ. Fig. 7 shows the relationships between initial rate coefficient (v_i) vs. χ at 400 nm and 25 °C. The kinetic analysis showed a rate coefficient value of 0.247 ± 0.006 with $R^2 = 0.996$ in the range of studied χ for [ChCl][Met] and of 0.833 ± 0.007 with $R^2 = 0.964$ in the range of studied χ for [ChCl][Pro]. Note that, [ChCl][Pro] is faster 3.5 times in comparison to [ChCl][Met] and the rate coefficient increases in the same order of χ. This fact is attributable a priori to the viscosity effect (see Fig. S14 in SM).

The comparison between Figs. 6 and 7 show that the hydrolysis reaction in presence of the enzyme for [ChCl][Met] is improved three (3) times while [ChCl][Pro] twelve (12) times. However, the performance of the reaction along the mixtures in presence of CALB is better in [ChCl][Pro] in comparison to [ChCl][Met]. This fact, would be explained based

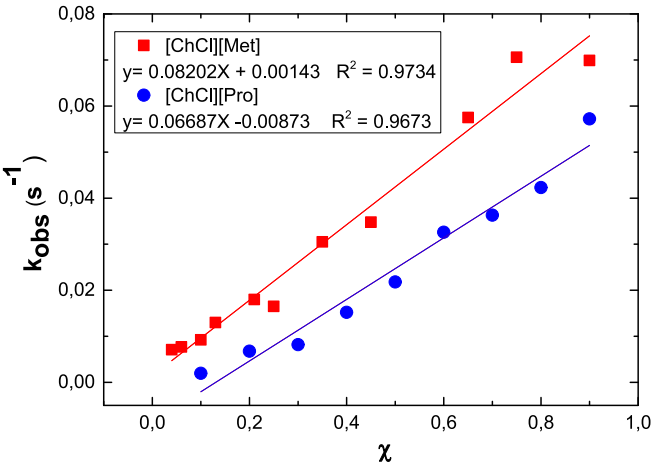

Fig. 6. Relationships between kinetic rate constants (k_{obs}) associated to the formation of *p*-NP vs. χ of [ChCl][Met]/water mixtures (full squares) and empty squares for [ChCl][Pro], respectively.

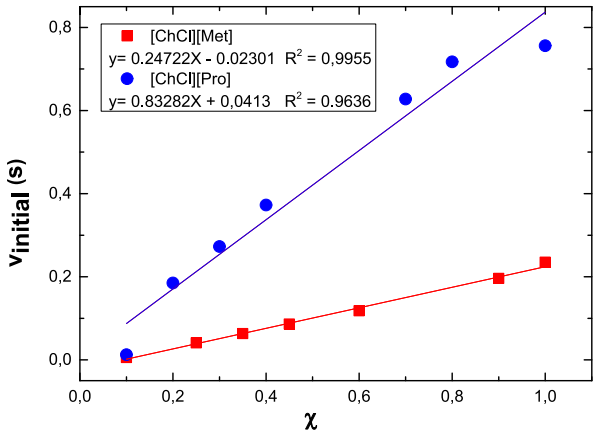

Fig. 7. Relationships between initial rate associated to formation of *p*-NP vs. χ of [ChCl][Met]/water mixtures (full squares) and empty squares for [ChCl][Pro], respectively in presence of CALB.

on the chemical structure of proline. This AA presents a rigid ring (pyrrolidine ring) conferring a rigid chemical structure (see Scheme 1 above). This feature will induce variations in the conformational arrangements of the protein (CALB) [53]. A suitable alternative for elucidating the mechanism by which the enzyme is activated-involving hydrophobic interactions with the ring structure of the amino acid, conformational rearrangements of CALB, and hydrogen bonding (HB) at the enzyme's active center-would be to supplement the experimental study with molecular dynamics (MD) simulations [54]. Nevertheless, the experimental work, if sufficiently comprehensive and detailed, can by itself provide strong evidence for activation patterns of the enzyme mediated by the reaction medium.

3.3.3. *Lineweaver-Burk relationships*

The Michaelis-Menten equation gives a hyperbolic dependence of the enzyme velocity (v) with the [S], where the K_M or substrate affinity constant is $K_M = \frac{(k_{-1}+k_2)}{k_1}$ and v_{max} is the maximum enzyme velocity ($v_{max} = k_2[E_T]$) achieved by the catalytic reaction at saturating [S] [55]. Then, the Michaelis-Menten equation is $v_0 = \frac{v_{max}[S]}{K_M+[S]}$. The catalytic efficiency $\left(\frac{k_{cat}}{K_M}\right)$ is defined by how efficiently an enzyme converts a S into P, when $k_2 = k_{cat} = \frac{v_{max}}{[E_T]}$. Therefore, the catalytic efficiency is $\frac{(k_2\, k_1)}{(k_{-1}+k_2)}$ [19,23]. The Lineweaver-Burk relationships were analyzed in three (3) aqueous mixtures for [ChCl][Met] ($\chi = 0.25$, $\chi = 0.65$ and $\chi = 0.85$, see Table 1 and Table S7 and Fig. S8 A in SM) and two (2) aqueous mixtures for [ChCl][Pro] ($\chi = 0.25$ and $\chi = 0.65$, see Table 2 and Table S8 and Fig. S8 B in SM for more details) to obtain the catalytic parameters (K_M and v_{max}), which are used in order to explore the kinetic behavior [19,23,32].

The k_{cat} parameter is defined as k_2 (ES→P) from Scheme S1 in SM. In agreement with this parameter, the mixture given by [ChCl][Met] ($\chi = 0.85$) showed the best trends to departure the product from the ES complex. K_M is associated to the bound strength of the ES complex (affinity constant denoted by K_M). Thus, the same mixture cited above ($\chi = 0.85$) shows a peak in comparison to the other mixtures, suggesting that

Table 1
Kinetic parameters determined in [ChCl][Met] and its aqueous mixtures for CALB and *p*-NPL at $\chi = 0.25$; 0.65 and 0.85, respectively.

χ	v_{max} (M/s)	K_M (M)	k_{cat} (s^{-1})	k_{cat}/K_M ($M^{-1}\ s^{-1}$)
0.25	0.035	0.40	35	87.50
0.65	0.140	1.61	140	86.96
0.85	0.160	1.87	162	86.63

Table 2
Kinetic parameters determined in [ChCl][Pro] and its aqueous mixtures for CALB and *p*-NPL at $\chi = 0.25$ and 0.60, respectively.

χ	v_{max} (M/s)	K_M (M)	k_{cat} (s^{-1})	k_{cat}/K_M ($M^{-1}\ s^{-1}$)
0.25	0.030	0.16	30	187.50
0.60	0.037	0.24	37	154.20

the best trend to departure the P from the ES complex will be that mixture given by [ChCl][Met]. The best catalytic efficiency $\left(\frac{k_{cat}}{K_M}\right)$ is located in [ChCl][Met] at $\chi = 0.25$. However, this parameter for [ChCl][Met] shows similar values. On the other hand, the best $\left(\frac{k_{cat}}{K_M}\right)$ is showed for [ChCl][Pro] at $\chi = 0.25$. This fact, will be explaining the observed behavior in Fig. 7 above.

For the aqueous mixture of [ChCl][Met] at $\chi = 0.85$, CALB reaches its best behavior. This is a mixture poor in water molecules and where its water should be surrounding the [ChCl][AA] will present a middle conductivity (see Fig. S13 in SM) and a high viscosity (Fig. S14 in SM). On the other hand, the ability to donate (β parameter, see Fig. 1 in the text) and accept (α parameter, see Fig. 2 in the text) HB is higher in comparison other mixtures denoting a zone strong in polarizability (See Fig. 3 in the text). At this mixture is suggested that should show strong interactions between HBD and HBA moieties proposing a [ChCl][AA] stablished. This fact was reinforced with the SFT analysis (see Fig. 6 in the text and Fig. 15 A in SM). Then, it is suggested a conformational stability given by a stabilized network of [ChCl][Met]. This information suggests that the best interaction between the substrate and the enzyme-active site is promoted by a more stable conformation where CALB acquires a more restrictive structure. This is an interesting point because recently Campodónico et al. [19] reported that CALB is improved in mixtures of DES rich in aqueous media. This find suggests a diverse nature of each DES and how its play a key role over the activity of CALB. Then, kinetic response is dependent of the bulk properties of the solvent. Note that, the solvent effects studies have been addressed experimentally in order to get detailed information about the phenomena that are not observable and occurring at microscopic level. A pertinent alternative will be integrated to a reliable molecular dynamics study in order to support the proposed explanation. Note that, recently was reported that CALB requires a reaction media rich in water molecules (aqueous mixture of choline chlorine urea (CU) at 25 %*w*/*w*) to improve the interaction between the substrate and the enzyme-active site [19]. The author suggests that the stablished interactions are able to influence to the enzyme to acquiree a determinate conformational arrangement highly stable by the reaction media and a key role of the water molecules at this mixture. However, this study shows that CALB in choline chlorine methionine at $\chi = 0.85$ reaches its best behavior. The only difference is that urea was changed by methionine. Urea is a polar molecule and it shows a high solubility in water (1.08 Kg/L) in comparison to methionine (0.01 Kg/L). Moreover, methionine is defined as an amphipathic molecule. Then, methionine can increase the catalytic rate of CALB in the hydrolysis of the *p*-NPL reaction at high χ_{MET}. The significant influence of methionine over CALB suggests that specific interactions will be occurring between them. Solvent effects parameters suggest that the low quantity of water molecules will be occluded in the [ChCl][AA] network, or these molecules will be externally solvating the [ChCl][AA] influencing the catalytic performance of the enzyme attributable to stable conformational arrangements and suggesting that the water molecules will be stablishing a solvation box close to the [ChCl][AA] formed. Note that, $\left(\frac{k_{cat}}{K_M}\right)$ is improved 4 times and k_{cat} 2893 times in [ChCl][Met] respect to CU at 25 % *w*/*w*; while $\left(\frac{k_{cat}}{K_M}\right)$ is improved 1.7 times and k_{cat} 2754 times in [ChCl][Pro] respect to CU at 25 % *w*/*w*.

Then, a significant catalytic effect is observed with reference to the same reaction, but in different reaction media. The observed solvent effects can be attributed to the HBD moiety in the [ChCl][AA], respectively. This HBD effect appears to be relative to HB interactions, chemical nature, enantiomeric form of the amino acid and polarizability allowed by the solvent over the bio-catalysis process.

4. Conclusions

This work presents a kinetic analysis of CALB in aqueous mixtures of two (2) [ChCl][AA]: [ChCl][Met] and [ChCl][Pro], respectively. The hydrolysis reaction of *p*-NPL was used as a model system to analyze the solvent effect over different compositions of each [ChCl][AA]. This study emphasizes the relevance of the solvent effects over a catalytic reaction opening a complete analysis that involves Kamlet y Taft parameters, physico-chemical parameters and kinetic studies.

The solvent parameters are suggesting that at the first region, rich in water molecules, the reactants that form the [ChCl][AA] are completely solvated with high formation of HB between them with the water molecules. As the [ChCl][AA] increases in composition of AA, is suggested that the water molecules are occluded in the [ChCl][AA] 3D-network or the water molecules are externally solvating the [ChCl][AA]. These finds are reinforced with the studied physicochemical parameters (conductivity and surface tension) that shown abrupt changes in their slopes, reflecting modifications in the nature of the mixtures.

The hydrolysis reaction of *p*-NPL without CALB in [ChCl][Met] is one order of magnitude higher in comparison to [ChCl][Pro], and the [phenolate form] increases with χ in agreement to the increase of [ChCl][AA] in the mixture. This fact suggests that [ChCl][AA] will participate in the reaction of phenoxide formation. On the other hand, this reaction with CALB shown that [ChCl][Pro] is faster 3.5 times in comparison to [ChCl][Met] and the rate values increases in the same order of χ. This fact was attributed to the rigid chemical structure of proline able to induces conformational changes in CALB. However, the Lineweaver-Burk relationships showed that the enzymatic reaction requires a reaction media rich in [ChCl][Met] ($\chi = 0.85$) able to promote low degree of freedom that determine a more stable conformation of CALB acquiring a more restrictive structure in comparison to mixtures rich in water molecules. Solvent effects parameters suggest that the low quantity of water molecules will be occluded in the [ChCl][AA] network or these molecules will be externally solvating the [ChCl][AA] influencing the catalytic performance of the enzyme attributable to stable conformational arrangements induced by the enantiomeric form of methionine and the water molecules will be stablishing a solvation box close to the [ChCl][AA] formed. The significance of this study and its broader implications are over applications and new perspectives of green industrial solvents in a biocatalysis process. This study corroborates the catalytic benefits of [ChCl][AA] as a reaction medium. However, it is important to note that its synthesis depends on high-purity amino acids, which can be costly. Therefore, developing a cost-effective preparation process is essential for large-scale applications. Additionally, industrial-grade CALB may contain impurities that could compromise the stability of [ChCl][AA], necessitating the optimization of enzyme pre-treatment methods. Subsequently, a new series of experiments should be undertaken to translate the findings of this study into industrial-scale production. Considerations for such scale-up include maintaining the characteristics of the synthesis in bulk volumes, evaluating the costs of reagents and enzymes, assessing the economic viability of solvent recyclability, determining the number of reuse cycles for both the enzyme and solvent, and evaluating the environmental impact.

CRediT authorship contribution statement

Paola R. Campodónico: Writing – review & editing, Writing – original draft, Visualization, Validation, Supervision, Software, Resources, Project administration, Methodology, Investigation, Funding acquisition, Formal analysis, Data curation, Conceptualization. **Karla Calfuman:** Methodology, Investigation, Formal analysis, Data curation. **Cristian Suárez-Rozas:** Methodology, Investigation, Formal analysis, Data curation. **Jackson J. Alcázar:** Writing – review & editing. **Belén Olivares:** Writing – review & editing.

Author statement

We confirm that the manuscript has been read and approved by all named authors and that there are no other persons who satisfied the criteria for authorship but are not listed. We further confirm that the order of authors listed in the manuscript has been approved by all of us. We understand that the Corresponding Author is the sole contact for the Editorial process (including Editorial Manager and direct communications with the office). She is responsible for communicating with the other authors about progress, submissions of revisions and final approval of proofs. We confirm that we have provided a current, correct email address which is accessible by the Corresponding Author.

Funding

This research received no external funding.

Declaration of competing interest

The authors declare that they have no known competing financial interests or personal relationships that could have appeared to influence the work reported in this paper.

Acknowledgments

PRC thanks to Fondecyt Grant #1241028 and Instituto de Ciencias e Innovación en Medicina (ICIM), Facultad de Medicina, Universidad del Desarrollo (UDD).

Appendix A. Supplementary data

Supplementary data to this article can be found online at https://doi.org/10.1016/j.molliq.2025.128862.

Data availability

Data will be made available on request.

References

[1] I. Pacheco-Fernández, V. Pino, Extraction with ionic liquids-organic compounds. In liquid-phase extraction; LPE, handbooks in Sep, Sci 17 (2020) 499–537, https://doi.org/10.1016/B978-0-12-816911-7.00017-7.
[2] P. Pavéz, R. Figueroa, M. Medina, D. Millán, R.D. Falcone, R. Tapia, Choline [amino acid] ionic liquid/water mixtures: a triple effect for the degradation of an organophosphorus pesticide, ACS Omega 5 (2020) 26562–26572, https://doi.org/10.1021/acsomega.0c03305.
[3] R.A. Sheldon, Biocatalysis and biomass conversion in alternative reaction media, Chem. Eur. J. 22 (2016) 12984–12999, https://doi.org/10.1002/chem.201601940.
[4] P.T. Anastas, J.C. Warner, Green chemistry: Theory and Practice. ISBN 10: 0198502346. Oxford University Press. New York, 1998.
[5] M. Poliakoff, P.T. Anastas, A principled stance, Nature 413 (2001) 257, https://doi.org/10.1038/35095133.
[6] J.S. Wilkes, A short history of ionic liquids—from molten salts to neoteric solvents, Green Chem. 4 (2002) 73–80, https://doi.org/10.1039/B110838G.
[7] T. Welton, Room-temperature ionic liquids. Solvents for synthesis and catalysis, Chem. Rev. 99 (2013) 2071–2084, https://doi.org/10.1021/cr980032t.
[8] T. Welton, Ionic liquids in green chemistry, Green Chem. 13 (2011) 225, https://doi.org/10.1039/c0gc90047h.
[9] H. Ohno, K. Fukumoto, Amino acid ionic liquids, Acc. Chem. Res. 40 (2007) 1122–1129, https://doi.org/10.1021/ar700053z.
[10] S. Kirchecker, D. Esposito, Amino acid based ionic liquids: a green and sustainable perspective, Curr. Opin. Green Sust. Chem. 2 (2016) 28–33, doi.org/10.1016/jcogsc.2016.09.001.

[11] B. Kanjilal, I. Noshadi, Bioionic liquids: enabling a paradigm shift toward advanced and smart biomedical applications, Adv. Intell. Syst. 5 (2023) 2200306–2200328, https://doi.org/10.1002/aisy.202200306.

[12] M. Taha, M.R. Almeida, F.A. Silva, P. Domínguez, S.P.M. Ventura, J.A.P. Coutinho, Novel biocompatible and self-buffering ionic liquids for biopharmaceutical applications, Chem. Eur. J. 21 (2015) 4781–4788, https://doi.org/10.1002/chem.201405693.

[13] J.M. Gomes, S.S. Silva, R.R. Reis, Biocompatible ionic liquids: fundamental behaviours and applications, Chem. Soc. Rev. 48 (2019) 4317–4335, https://doi.org/10.1039/c9cs00016j.

[14] N. Gaikwad, S. Kudal, A.M. Avachat, Choline-amino acid-derived bio-ionic liquids for solubility enhancement of Zafirlukast, AAPS Pharm. Sci. Tech. 23 (2022) 146–159, https://doi.org/10.1228/s12249-022-02296-8.

[15] M. Petkovic, J.L. Ferguson, H.H.Q.N. Gunaratne, R. Ferreira, M.C. Leitao, K. R. Seddon, Nobel biocompatible cholinium-based ionic liquids-toxicity and biodegradability, Green Chem. 12 (2010) 643–649, https://doi.org/10.1039/b922247b.

[16] A. Paiva, R. Craveiro, I. Aroso, M. Martins, R.L. Reis, A.R.C. Duarte, Natural deep eutectic solvents – solvents for the 21st century, ACS Sust. Chem. Engn. 2 (2014) 1063–1071, https://doi.org/10.1021/sc500096j.

[17] Q. Zhang, K. De Oliveira Vigier, S. Royer, F. Jérôme, Deep eutectic solvents: syntheses, properties and applications, Chem. Soc. Rev. 41 (2012) 7108–7146, https://doi.org/10.1039/c2cs35178a.

[18] B. Sánchez, P.R. Campodónico, R. Contreras, Gutmann's donor and acceptor numbers for ionic liquids and deep eutectic solvents, Front. Chem. 10 (2022) 861379, https://doi.org/10.3389/fchem.2022.861379.

[19] P.R. Campodónico, J. Alarcón-Espósito, J.J. Alcázar, B. Olivares, C. Suárez-Rozas, Analysis of the behavior of deep eutectic solvents upon addition of water: its effects over a catalytic reaction, Molecules 29 (2024) 3296–3311, https://doi.org/10.3390/molecules29143296.

[20] R. Giernoth, Task-specific ionic liquids, Angew. Chem. Int. Ed. Eng. 49 (2010) 2834–2839, https://doi.org/10.1002/anie.200905981.

[21] W. Zhuang, K. Hachem, D. Bokov, M.J. Ansari, A.T. Nakhjiri, Ionic liquids in pharmaceutical industry: a systematic review on applications and future perspectives, J. Mol. Liq. 349 (2022) 118145–118153, https://doi.org/10.1016/j.molliq.2021.118145.

[22] Z. Usmani, M. Sharma, P. Gupta, Y. Karpichev, N. Gathergood, R. Bhat, V.K. Gupta, Ionic liquid based pretreatment of lignocellulosic biomass for enhanced bioconversion, Bioresour. Technol. 304 (2020) 123003, https://doi.org/10.1016/j.biortech.2020.123003.

[23] P.R. Campodónico, C. Calderón, J.J. Alcázar, B. Olivares, L. Jaldin, C. Suárez-Rozas, Exploring the behavior of Candida antarctica lipase B in aqueous mixtures of an imidazolium ionic liquid and its surfactant analogue, Front. Chem. 11 (2024), https://doi.org/10.3389/fchem.2023.1289398.

[24] C.M.A.P. Schuh, F. Ezquer, S. Mamani, P.R. Campodónico, C. Cárcamo, F. Martinez-Gómez, I. Aburto, M. Ezquer, B. Morales, B. Olivares, A natural deep eutectic solvent as an effective material for dual debridement and antibiofilm effects in chronic wound treatment, Int. J. Pharm. 663 (2024) 124553–124565, https://doi.org/10.1016/j.ijpharm.2024.124553.

[25] D. Mondal, M. Sharma, M.V. Quental, A.P.M. Tavares, K. Prasad, M.G. Freire, Suitability of bio-based ionic liquids for the extraction and purification of IgG antibodies, Green Chem. 18 (2016) 6071–6081, https://doi.org/10.1039/C6GC01482H.

[26] G. Singh, M. Kaur, D. Singh, A.K. Kesavan, T.S. Kang, Antimicrobial colloidal complexes of lysozyme with bio-based surface active ionic liquids in aqueous medium, J. Phys. Chem. B 124 (2020) 3791–3800, https://doi.org/10.1021/acs.jpcb.0c00339.

[27] S. Kapre, S.S. Palakurthi, A. Jain, S. Palakurthi, DES-igning the future of drug delivery: a journey from fundamentals to drug delivery applications, J. Mol. Liq. 4 (2024) 305–321, https://doi.org/10.1016/jmoliq.2024.124517.

[28] Q.-P. Liu, X.-D. Hou, N. Li, M.-H. Zong, Ionic liquids from renewable biomaterials: synthesis, characterization and application in the pretreatment of biomass, Green Chem. 14 (2012) 304–307, https://doi.org/10.1039/C2GC16128A.

[29] L. Gontrani, Choline-amino acid ionic liquids: past and recent achievements about the structure and properties of these really "green" chemicals, Biophys. Rev. 10 (2018) 873–880, https://doi.org/10.1007/s12551-018-0420-9.

[30] A. Jordan, A. HaiB, M. Spulak, Y. Karpichev, K. Kümmerer, N. Gathergood, Synthesis of a series of amino acid derived ionic liquids and tertiary amines: green chemistry metrics including microbial toxicity and preliminary biodegradation data analysis, Green Chem. 18 (2016) 4374–4392, https://doi.org/10.1039/C6GC00415F.

[31] S.S. Silva, D.O. Abranches, A.S. Pinto, B.P. Soares, H. Passos, A.M. Ferreira, J.A. P. Coutinho, Solubility enhancement of hydrophobic compounds in aqueous solutions using biobased solvents as Hydrotropes, I&EC Res. 62 (2023) 12021–12028, https://doi.org/10.1021/acs.iecr.3c01469.

[32] C. Calderón, R. Contreras, P.R. Campodónico, Surfactant-mediated enzymatic superactivity in water/ionic liquid mixtures, evaluated on a model hydrolytic reaction catalyzed by α-chymotrypsin, J. Mol. Liq. 283 (2019) 522–531, https://doi.org/10.1016/j.molliq.2019.03.106.

[33] J. Uppenberg, M.T. Hansen, S. Patkar, T. Jones, The sequence, crystal structure determination and refinement of two crystal forms of lipase B from *Candida antarctica*, Struct 2 (1994) 293–308.

[34] R. P. D. Bank, Rcsb Pdb—1tca: The Sequence, Crystal Structure Determination and Refinement of Two Crystal Forms of Lipase b from *Candida antarctica*, Available online: https://www.rcsb.org/structure/1tca (accessed on january, 2025.

[35] J.A. Laszlo, D.L. Compton, α-chymotrypsin catalysis in imidazolium-based ionic liquids, Biotechnol. Bioeng. 75 (2001) 181–186, https://doi.org/10.1002/bit.1177.

[36] X. Ma, Y. Li, Q. Zhou, G. Zhu, J. Xiong, L. Zhao, X. Yang, S. Wang, Green amino acid ionic liquids-based aqueous biphasic systems for efficient extraction of gold (I) from alkaline solution, Ind. Eng. Chem. Res. 62 (2023) 15226–15239, https://doi.org/10.1021/acs.iecr.3c02705.

[37] E.A. Castro, P.R. Campodónico, A. Toro, J.G. Santos, Kinetics and mechanism of the aminolysis of 4-methylphenyl and 4-chlorophenyl 2,4-dinitrophenyl carbonates in aqueous ethanol, J. Organomet. Chem. 68 (2003) 5930–5935, https://doi.org/10.1021/jo034385q.

[38] P.R. Campodónico, B. Olivares, R. Tapia, Experimental Analyses Emphasize the Stability of the Meisenheimer Complex in a S_NAr Reaction toward trends in Reaction Pathways, Front. Chem. 8 (2020), https://doi.org/10.3389/fchem.2020.00583.

[39] M.M. Nolasco, S.N. Pedro, C. Vilela, P.D. Vaz, P. Ribeiro-Claro, S. Rudic, S. F. Parker, C.S. Freire, M.G. Freire, A.J.D. Silvestre, Water in deep eutectic solvents: new insights from inelastic neutron scattering spectroscopy, Front. Phys. 10 (2022) 834571, https://doi.org/10.3389/fphy.2022.834571.

[40] F. Gabriele, M. Chiarini, R. Germani, M. Tiecco, N. Spreti, Effect of water addition on choline chloride/glycol deep eutectic solvents: characterization of their structural and physicochemical properties, J. Mol. Liq. 291 (2019) 111301–111307, https://doi.org/10.1016/j.molliq.2019.111301.

[41] C. Reichardt, Polarity of ionic liquids determined empirically by means of Solvatochromic Pyridinium N-phenolate betaine dyes, Green Chem. 7 (2005) 339–351, https://doi.org/10.1039/B500106B.

[42] S.L. Sherman, K.C. Fisher, E. Garand, Effects of methyl side chains on the microsolvation structure of protonated tripeptides, J. Phys. Chem. A 127 (2023) 6275–6281, https://doi.org/10.1021/acs.jpca.3c03711.

[43] R.W. Taft, M.J. Kamlet, The solvatochromic comparison method. 2. The alpha -scale of solvent hydrogen -bond donor (HBD) acidities, J. Am. Chem. Soc. 98 (1976) 2886–2894, https://doi.org/10.1021/ja00426a036.

[44] M.J. Kamlet, R.W. Taft, The solvatochromic comparison method. I. The beta -scale of solvent hydrogen -bond acceptor (HBA) basicities, J. Am. Chem. Soc. 98 (1976) 377–383, https://doi.org/10.1021/ja00418a009.

[45] M.J. Kamlet, J.L.M. Abboud, M.H. Abraham, R.W. Taft, A comprehensive collection of the solvatochromic parameters, π^*, α, β, and some methods for simplifying the generalized solvatochromic equation, J. Organomet. Chem. 48 (1983) 2877–2887, https://doi.org/10.1021/jo00165a018.

[46] J.D. Andrade, L.M. Smith, D.E. Gregonis, The contact angle and Interface energetics, in: J.D. Andrade (Ed.), Surface and Interfacial Aspects of Biomedical Polymers, Springer, Salt Lake City, Utah, 1985, pp. 249–292.

[47] Y. Chen, W. Chen, L. Lu, Y. Yang, Y. Wang, X. Hu, F. Wang, T. Mu, Surface tension of 50 deep eutectic solvents: effect hydrogen-bonding donors, hydrogen-bonding acceptors, others solvents and temperature, Ind. Chem. Res. 58 (2019) 12741–12750, https://doi.org/10.1021/acs.iecr.9b00867.

[48] Y. Rublova, A. Kityk, F. Danilov, V. Protsenko, Mechanistic study on surface tension of binary and ternary mixtures containing choline chloride, ethylene glycol and water components of aqueous solutions of a deep eutectic solvent, ethaline, Z. Phys. Chem. 234 (2020) 399–413, https://doi.org/10.1515/zpch-2019-1492.

[49] F.O. Farias, H. Passos, J.A.P. Coutinho, M.R. Mafra, pH effect on the formation of deep eutectic solvent based aqueous two-phase systems, Ind. Eng. Chem. Res. 57 (2018) 16917–16924, https://doi.org/10.1021/acs.iecr.8b04256.

[50] R.C. Gaioto, M.C.G.C. Dias, P.M. Ndiaye, L. Igarashi-Mafra, M.R. Mafra, Choline chloride aqueous solution: a thermophysical study, Fluid Phase Equilib. 574 (2023) 113903–113915, https://doi.org/10.1016/j.fluid.2023.113003.

[51] H.K.M. Salomaki, P. Vainikka, E. Makila, F. Poletti, S. Ruggeri, F. Terzi, J. Lukkari, Effect of water on a hydrophobic deep eutectic solvent, J. Phys. Chem. B 126 (2022) 513–527, https://doi.org/10.1021/acs.jpcb.1c08170.

[52] Determining and Calculating pH, Available at: https://chem.libretexts.org/Bookshelves/Physical_and_Theoretical_Chemistry_Textbook_Maps/Supplemental_Modules_(Physical_and_Theoretical_Chemistry)/Acids_and_Bases/Acids_and_Bases_in_Aqueous_Solutions/The_pH_Scale/Determining_and_Calculating_pH, 2020.

[53] X.-G. Zhang, Y. Xue, Z.-P. Lu, H.-J. Xu, Y. Hu, Chemical Modification for Improving Catalytic Performance of Lipase B from *Candida Antarctica* with Hydrophobic Proline Ionic Liquid, Bioprocess Biosyst. Eng. 45 (2022) 749–759, https://doi.org/10.1007/s00449-022-02696-x.

[54] Q. Qiao, J. Shi, Q. Shao, Effect of water on solvation and structure of lipase in deep eutectic solvents containing protein destabilizer and stabilizer, Phys. Chem. Chem. Phys. 23 (2021) 23372–23379, https://doi.org/10.1039/D1CP03282H.

[55] L. Michaelis, M.L. Menten, Die Kinetik der Invertinwirkung. Biochem. Z. 49 (1913) 333–369.